Appl. Phys. B 59, 1–9 (1994)

Applied Physics B Lasers and Optics

Spectroscopic studies of laser-produced plasmas formed in CO and CO_2 using 193, 266, 355, 532 and 1064 nm laser radiation

J.B. Simeonsson*, A.W. Miziolek

US Army Research Laboratory, AMSRL-WT-PC, Aberdeen Proving Ground, MD 21005-5066, USA
(Fax: +1-410/278-6150)

Abstract. The wavelength dependence of laser-produced breakdown in air, CO and CO_2 has been studied using the four Nd:YAG harmonics (266 nm, 355 nm, 532 nm and 1064 nm) and the ArF-excimer laser (193 nm). Breakdown thresholds at these wavelengths are reported for air, CO and CO_2. A significant reduction in the breakdown thresholds for both CO and CO_2 is apparent when comparing 193 nm with the four Nd:YAG harmonics. This reduction is attributed to the resonance-enhanced two-photon ionization of metastable carbon atoms generated in the laser focus at the ArF-laser wavelength. In addition to reporting breakdown thresholds, the laser-produced plasmas in CO and CO_2 are characterized in terms of plasma temperatures and electron densities which are measured by time-resolved emission spectroscopy. Electron densities range from 9×10^{17} cm^{-3} to 1×10^{17} cm^{-3}. Excitation temperatures range from 22 000 K at 0.2 μs to 11 000 K at 2 μs. Ionization temperatures range from 22 000 K at 0.1 μs to 16 000 K at 2 μs. Evidence is presented to indicate that, like ArF-laser-produced plasmas, Nd:YAG-laser-produced plasmas formed in CO and CO_2 are in or near a state of Local Thermodynamic Equilibrium (LTE) soon after their formation.

PACS: 52.25.Qt, 52.25.Rv, 52.50.Jm

Laser-induced breakdown in gases continues to be a subject of active theoretical and experimental study [1–3]. There is particular interest of late in using laser-produced plasmas for elemental and molecular analysis of various sample media [4–9]. Among the attractive features of laser-produced plasma methods are direct sampling with minimal sample preparation, versatile sampling of all media, and speed of analysis. With the wide range of potential analytical applications these plasmas are likely to find, there are as yet to be reported detailed spectroscopic studies of laser-produced plasmas formed in gases, particularly as a function of the laser wavelength.

At infrared wavelengths, laser-induced breakdown is generally understood to occur by an avalanche ionization mechanism in which the initial "seed" electron(s) is produced either by multiphoton ionization or thermal processes. The seed electrons absorb energy from the laser and distribute it to the gas through collisions leading to heating, further ionizations and ultimately breakdown of the gas. At wavelengths less than 1 micron, laser-induced breakdown in a gas is believed to occur by way of multiphoton ionization and collisional/avalanche ionization processes [1, 3, 10–12]. The relative importance of the two ionization processes depends on the laser wavelength, the presence of any spectral resonances with the gas species and the pressure of the gas. In the absence of spectral absorption resonances, collisional (avalanche) ionization dominates at higher pressures and longer (near IR to IR) wavelengths. Conversely at shorter wavelengths (visible to ultraviolet) and low pressure, photoionization becomes increasingly important [10].

To further the development of laser-produced plasmas as spectrochemical sources, we have initiated a series of studies of these plasma environments. Recently we reported the results of time-resolved emission studies of ArF-laser-produced plasmas formed in CO, CO_2, methanol and chloroform gases [13]. It was shown that ArF-laser-induced breakdown occurs in carbon containing gases at unusually low irradiances. Although the breakdown thresholds appeared to vary considerably with the changes in chemical structure of the precursor species, no differences in the temperature or density characteristics of the resulting plasma environments were observed. It has been proposed that a spectral overlap of the ArF-laser output at 193 nm with the $2p3s\ ^1P_1 \leftarrow 2p^2\ ^1D_2$ transition of carbon at 193.093 nm increases the initial photoionization rate resulting in a lower threshold for breakdown for carbon bearing molecules. However, it has yet

* NRC/ARL Postdoctoral Research Associate and author to whom all correspondence should be addressed.

Present address: Department of Chemistry, University of Iowa, Iowa City, IA 52242-1294, USA

to be shown in a single study that the threshold at this wavelength is significantly lower than at other wavelengths throughout the ultraviolet, visible to near infrared regions.

In the work reported here, spectroscopic studies have been extended to laser-produced plasmas formed in CO and CO_2 gases using 266 nm, 355 nm, 532 nm and 1064 nm radiation for the purpose of determining a wavelength dependence of the intensity breakdown thresholds and also to determine characteristic plasma temperatures and electron densities. All of the emission measurements are line-of-sight and therefore represent spatially averaged values of temperature or density. The thermodynamic equilibrium status of the plasmas has been considered in order to validate the use of spectroscopic methods of temperature evaluation. Current results are compared with those of previous studies, including our previous studies of ArF-laser-produced plasmas in CO and CO_2, to demonstrate wavelength dependent characteristics of laser-produced plasma environments.

1 Experimental

A Nd:YAG laser (Quanta Ray, DCR-1A) was used as the excitation source in these studies and provided up to 40 mJ at 266 nm, 125 mJ at 355 nm, 400 mJ at 532 nm and 800 mJ at 1064 nm. Comparison measurements at 193 nm employed a Lambda Physik 105i ArF-excimer laser with the same supporting instrumentation. Details of that system were reported previously in [13]. The output from the laser(s) was directed by prisms to a lens of focal length 10 cm which focused the laser beam just above the end of a flow tube (i.d. 1.4 mm) through which CO and CO_2 gases were flowed (150 cm^3/min). The flow tube was positioned concentrically inside of a larger flow tube (i.d. 9 mm) through which helium was flowed (1 l/min) in order to sheath the plasma region from room air. The helium sheath was important for isolating the breakdown region from dust or aerosol particles which could lead to artificially low breakdown thresholds. A calorimeter (Scientech, with either ultraviolet or visible/infrared sensitive surfaces) used to measure the laser energy transmitted by the plasma also served as a beam dump.

Plasma emissions were collected perpendicular to the laser beam axis by a quartz lens (focal length 25 cm) and imaged without magnification onto the entrance slit of a spectrometer (0.5 m focal length, SPEX-500, SPEX Industries). Detection was accomplished using two PhotoMultiplier Tubes (PMTs) (9826-Q, UV sensitive and 9658B, IR sensitive, Thorn EMI). The anode output was sampled by a boxcar averager (Stanford Research Systems, SR-250) triggered by a fast photodiode (Hamamatsu) that was placed near the output of the YAG laser. The output of the boxcar was directed to a PC (Zenith Data Systems) for data collection and storage. The output from the PMT was also directed to an oscilloscope (Tektronix 2460) for real-time monitoring of the plasma decay for optimization of the timing.

Wavelength scans of the oxygen and carbon neutral and ion plasma emissions were performed at a constant time delay relative to the laser pulse (which corresponded to time zero). Time delays were selected by advancing the boxcar gate in 100 ns (prior to 1 μs) and 200 ns (after 1 μs) increments. The wavelength response of the optical detection system was measured using a calibrated standard lamp (Eppley Laboratory, Serial no. EPT-1293). For some measurements, the plasma emissions were attenuated by neutral density filters (Melles Griot) placed before the entrance slits to avoid saturation of the PMT. When observing the emissions above 700 nm, it was necessary to place a long-pass filter (GG-455, Schott Filter Glass) in front of the entrance slit of the spectrometer to reject second-order transmission of the plasma.

Laser pulse energies used to produce the laser plasmas were nominally 10–20 mJ, depending on the wavelength employed. The pulse energy was kept as near as possible to the breakdown threshold to maintain near threshold conditions in the plasmas, but was also held high enough to insure consistent and reproducible breakdown plasma formation in the gas. This usually occurred at pulse energies that were no more than 10% greater than the pulse energy threshold for breakdown in air. While the dimensions of the plasmas were not measured, they were observed visually to be of approximately the same size, with the exception of the 1064 nm plasmas which were noticeably larger. The relative sizes were consistent with the amount of energy estimated to be deposited into the plasmas, as determined by the difference of the incident and transmitted laser energies (see Table 1).

The pulse widths of the Nd:YAG laser were measured using a fast photodiode (risetime < 200 ps, falltime < 350 ps, model ET2000, Electro-Optics Technology). Pulse widths, used to determine incident laser intensities, were 8, 7 and 7 ns (FWHM) at 1064 nm, 532 nm and 355 nm, respectively, and are similar to those reported by Davis et al. [3]. Due to the limited spectral response of the photodiode, the laser pulse width could not be measured at 266 nm and was assumed to be no greater than 7 ns. It is important to note that the measured pulse

Table 1. Incident Laser Energies (ILE), Transmitted Laser Energies (TLE) and maximum deposited energies (E_{dep}) for CO and CO_2 at 193 nm, 266 nm, 355 nm, 532 nm and 1064 nm

Wavelength [nm]		ILE [mJ]	TLE [mJ]	E_{dep} [mJ] max
193	CO	10	6	4
193	CO_2	10	7.5	2.5
266	CO	10.7	8.2	2.5
266	CO_2	10.2	7.4	2.8
355	CO	10.4	7.1	3.3
355	CO_2	10.1	6.6	3.5
532	CO	9.3	6.5	2.8
532	CO_2	11.5	7	4.5
1064	CO	16	10	6
1064	CO_2	21	14	7

widths are average values and do not account for the true output of the Nd:YAG laser which is characterized by high intensity spikes within the observed laser pulse envelope. It is likely that the spikes in the laser pulse profile provide the intensity necessary for breakdown to occur. Thus, the breakdown thresholds reported using the average pulsewidths are expected to be less than the actual threshold values. Breakdown thresholds were determined from the average of several pulses, nominally 1000 at 10 Hz.

The beam waist diameters of the focused laser beam were measured by passing a razor edge through the laser focus. The razor edge was mounted onto a translation stage with micrometer positioning adjustors. The estimated areas of the focal spot at 266 nm, 355 nm, 532 nm and 1064 nm ranged from 3.2×10^{-5} cm^2 to 1.1×10^{-4} cm^2 and are within a factor of two of those reported previously using the same laser and lens combination [3]. The ArF laser employed unstable resonator optics ensuring good focal characteristics. The raw laser beam of the ArF laser had a rectangular shape (0.6 cm × 2.5 cm) which was apertured to an approximately circular shape of diameter 6 mm. With a 10 cm focal length lens, the focal diameter of the ArF laser is measured (using the razor-blade edge) to be 90 μm giving an estimated focal area of 6.2×10^{-5} cm^2.

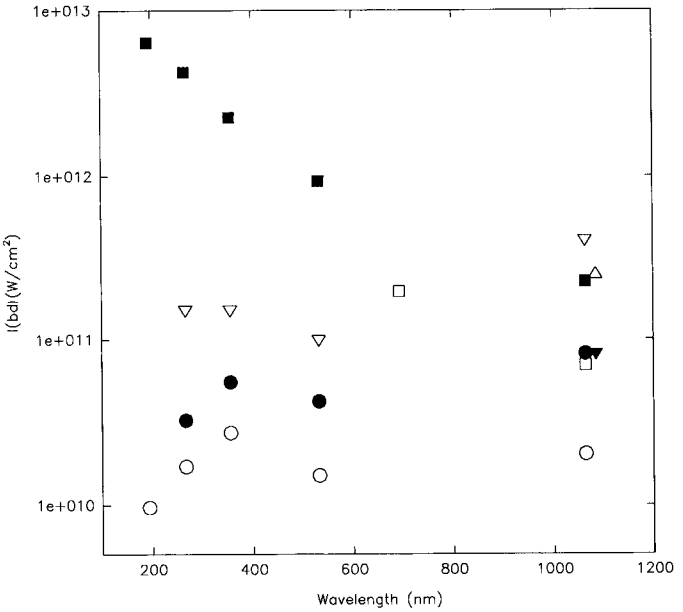

Fig. 1. Plot of the intensity breakdown thresholds, I_{bd} (in W/cm^2), in air and nitrogen as a function of the laser wavelength. *Open circles:* air this study; *filled circles:* air from [3]; *open squares:* air [10]; *filled squares:* air model [10]; *open inverted triangles:* air [14]; *filled inverted triangle:* air [17]; *open triangle:* air [18]

2 Results

At breakdown, the laser-produced plasma environment is spectroscopically characterized by strong continuum emission. Following the laser pulse, the plasma cools rapidly resulting in a decrease in the continuum emission and the appearance of strong neutral and ionic emissions of elemental species in the plasma [7]. The ionic emissions typically decay more rapidly (within a few microseconds) due to recombination processes with free electrons. Neutral emissions, including emissions from mono- and diatomic species, can last up to several microseconds [4, 15, 16]. As has been noted, the elemental and molecular emissions in the plasma environment are characteristic of the precursor species and can be used for chemical analysis, e.g., the Laser Microplasma Gas Chromatography Detector (LM-GCD) [15, 16], detection of Be in aerosols [4], and the detection of elemental pollutants in the atmosphere [5].

2.1 Breakdown intensity thresholds

Since the earliest observations of laser-induced breakdown in gases, much consideration has been given to the laser intensity required for breakdown [1, 3, 10–12]. The optical breakdown threshold, I_{bd}, is a function of the gas pressure, the ionization potential of the gas and the pulse width of the laser [10, 11]. Shown in Fig. 1 is a plot of the intensity breakdown thresholds for laser-produced plasmas formed in air or nitrogen at a pressure of 1 atm at various wavelengths. The plot includes experimental values reported previously in references [3, 10, 14, 17, 18] and values estimated using an expression from [10] that estimates the breakdown threshold intensity in air at 1 atm as a function of laser wavelength. In this study, the breakdown threshold was taken to be the lowest laser intensity at which breakdown was observed visually in greater than 90% of the laser shots.

In general, it is difficult to compare breakdown thresholds directly from the literature as experimental parameters are rarely the same. Differences in laser output characteristics (beam quality, pulsewidth, dimensions) often result in significant variations in the observed thresholds. The experimental parameters (laser model, pulsewidth, beam dimensions, lens focal length) of the current study are nearly identical to those of Davis et al. [3], thus it should be possible to compare the thresholds measured in both studies to confirm the values of I_{bd} independently. Although the values reported in this study are consistently lower than those reported by Davis et al. [3], they are within a factor of four or better and the agreement is good as compared to the other experimental values shown in Fig. 1.

A comparison of thresholds measured in this study (open circles) with those calculated using the expression given by Smith and Meyerand [10] (filled squares), however, shows significant differences. While the model adequately predicts the threshold at 1064 nm, the agreement with experimentally measured values is increasingly poor at shorter wavelengths. The failure of the expression to reasonably predict the breakdown threshold is not surprising since the model assumes cascade ionization dominated conditions, which are less appropriate at shorter wavelengths. The divergence of experiment from theory illustrates the difficulty that is encountered in attempting

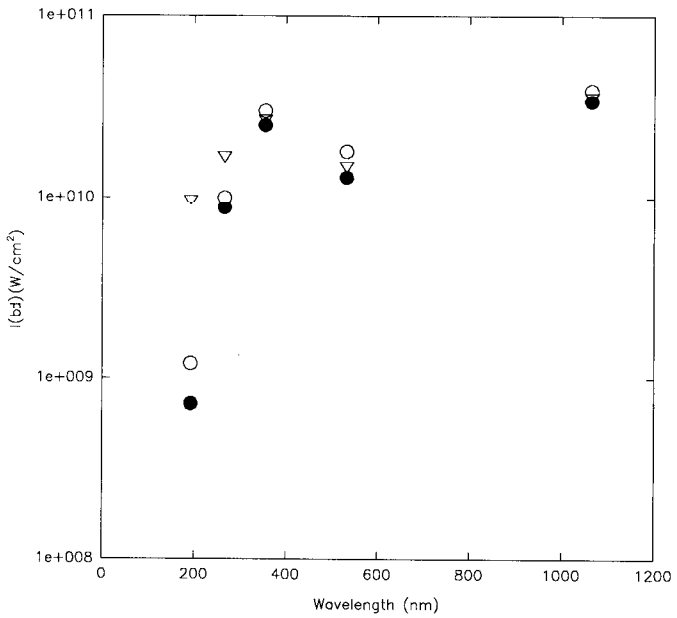

Fig. 2. Plot of the intensity breakdown thresholds, I_{bd} (in W/cm^2), in air, CO and CO_2 this work. Air: *open inverted triangles;* CO: *filled circles;* CO_2: *open circles*

to model the breakdown mechanism in this spectral region where the importance of quantum effects and photoionization increases with laser photon energies that approach the ionization energy of the gas [10].

It has been observed previously that I_{bd} is significantly reduced at 193 nm (ArF laser) relative to other wavelengths for carbon containing gases. It has been proposed [13, 15, 16] that the unusually low thresholds observed are due to the spectral overlap of the ArF-laser output (192.9–193.6 nm) with the $2p3s\ ^1P_1 \leftarrow 2p^2\ ^1D_2$ (61982–10194 cm^{-1}) transition of carbon at 193.093 nm [19–21]. One method of determining a resonance enhancement is to evaluate the wavelength dependence of the breakdown threshold in a carbon containing gas. Shown in Fig. 2 are the intensity thresholds for breakdown in CO, CO_2 and air at 193 nm and at 266 nm, 355 nm, 532 nm and 1064 nm. Direct comparisons of the results in this study in different gases at the various wavelengths are expected to be valid as the focusing lens, laser beam diameter and laser pulsewidth were made as nearly the same as possible.

While the breakdown thresholds for CO and CO_2 are nearly the same as for air at 266 nm, 355 nm, 532 nm and 1064 nm, there is a significant reduction in the thresholds at 193 nm. The reduction is almost certainly due to the resonance-enhanced two-photon ionization of carbon atoms produced in the laser focus which enables the critical ion/electron density to be achieved more rapidly. This is especially evident in I_{bd} for CO and CO_2 at 193 nm (remeasured for this study) which are at least an order of magnitude lower than thresholds for the same gases at the Nd:YAG laser wavelengths, and also by the corresponding laser pulse energies for breakdown at 193 nm, which were 450 μJ and 750 μJ for CO and CO_2, respectively, versus several mJ at each of the Nd:YAG

Table 2. I_{bd} (in W/cm^2) for CO, CO_2 and air gases at 193 nm, 266 nm, 355 nm, 532 nm and 1064 nm

Wavelength [nm]	CO	CO_2	Air
193	7.3×10^8	1.2×10^9	9.7×10^9
266	8.6×10^9	1.0×10^{10}	1.7×10^{10}
355	2.5×10^{10}	3.0×10^{10}	2.7×10^{10}
532	1.3×10^{10}	1.8×10^{10}	1.5×10^{10}
1064	1.9×10^{10}	2.2×10^{10}	2.0×10^{10}

wavelengths. By comparison, the laser pulse energy required for breakdown of air (primarily N_2 and O_2) at 193 nm was 6 mJ, approximately one order of magnitude greater. Table 2 is a compilation of the values of I_{bd} determined in this study for air, CO and CO_2 at 193 nm, 266 nm, 355 nm, 532 nm and 1064 nm. The apparent discrepancy between the breakdown thresholds for CO and CO_2 reported here and those reported previously in [13] is due to the fact that the beam waist diameter has been measured in this study (rather than estimated as previously in [13]). The difference in areas (measured versus estimated) is approximately one order of magnitude which accounts for most of the difference in the thresholds.

Another example of resonance enhancement in I_{bd} is seen in the thresholds for CO and CO_2 which show very close agreement at all wavelengths except at 193 nm. The lower threshold of CO at 193 nm is likely due to an efficient two-photon dissociation process [22]. The photodissociation of CO generates a high density of carbon and oxygen atoms in the laser focus which increases the initial ionization rate and consequently lowers I_{bd}.

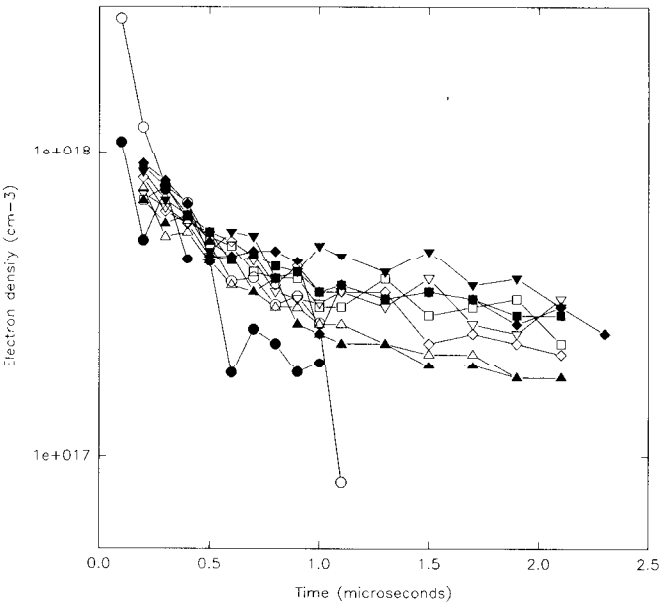

Fig. 3. Plot of the electron density as a function of time in laser-produced plasmas formed in CO and CO_2 gases. *Open symbols:* CO; *filled symbols:* CO_2. *Circles:* 193 nm; *inverted triangles:* 266 nm; *squares:* 355 nm; *triangles:* 532 nm; *diamonds:* 1064 nm

2.2 Electron density

Shown in Fig. 3 is a plot of the electron density of the Nd:YAG laser and ArF-laser plasmas formed in CO and CO_2 as a function of the plasma decay time. Electron densities at 193 nm are taken from [13]. The densities were evaluated from the Stark broadened emission profiles (corrected for Doppler and instrumental broadening) of the oxygen atom (neutral) emission at 844.65 nm $2p^3 3p\ ^3P \leftarrow 2p^3 3s\ ^3S$ (88631–76795 cm^{-1}) according to methods described by Griem and by Wiese [23, 24]. The magnitude of the electron densities ranges from 10^{17}–10^{18} cm^{-3} and is consistent with ranges reported previously [4, 13, 25]. Despite significant differences in the breakdown threshold energies and in the energies deposited at the various wavelengths, there is good agreement of the densities as a function of the plasma lifetime, both in different plasma gases (agreement between CO and CO_2 in all cases) and for all of the wavelengths studied. This is evidenced in the maximum electron density achieved early in the plasma lifetime and also in the magnitude of the electron density throughout the decay profile. The agreement indicates that in this pressure and laser intensity regime, the plasma electron density does not show an obvious spectral dependence. It also indicates that there is no observable chemical dependence of the electron density, as reported previously [13].

It is useful to compare the current results with those reported previously. Radziemski et al., who have performed numerous studies of laser produced plasmas formed in air, have reported electron densities ranging from 9×10^{17} cm^{-3} to 5×10^{16} cm^{-3} (0.2–10 μs) for plasmas formed at 580 Torr using a Nd:YAG laser at 1064 nm [4]. For air plasmas formed using a CO_2 laser at 10.6 μm, Radziemski et al. have reported electron densities ranging from 3.6×10^{17} cm^{-3} to 3.8×10^{16} cm^{-3} (1–25 μs) [25]. Stricker and Parker have reported peak electron densities (measured in the first 15–20 ns) of approximately 2×10^{18} cm^{-3} [17]. The results of the current study are consistent with each of these previous studies.

Measurements of the electron density are important for establishing the nature of the laser-produced plasma environment. The electron density ($10^{17} - 10^{18}$ cm^{-3}) observed suggests Local Thermodynamic Equilibrium (LTE) conditions can be expected. This is important if the methods used for evaluation of the temperature assume equilibrium distributions, i.e., spectroscopic measurements of the excitation and ionization temperature. The significance of the electron density and arguments for the existence of LTE will be presented in a later section.

2.3 Excitation temperature

Shown in Fig. 4 is a plot of the excitation temperatures (T_{exc}) in Nd:YAG and ArF-laser plasmas as a function of the plasma decay time. Temperatures shown at 193 nm using the ArF laser are taken from [13]. The excitation temperatures were determined from the integrated emissions of oxygen atoms (neutral) at 777 nm ($2p^3 3p\ ^5P \leftarrow 2p^3 3s\ ^5S$) (86629–73768 cm^{-1}) and 795 nm $2p^3 3p'\ ^3F \leftarrow 2p^3 3s'\ ^3D$) (113719–101143 cm^{-1}), as before [13]. There is close agreement of the temperatures between plasmas produced in CO and CO_2 gases (no observable chemical dependence) and also at all wavelengths studied. The excitation temperatures initially reach temperatures as high as 22 000 K but decrease and stabilize after 0.5 μs at approximately 14 000–16 000 K, except in the case of the 1064 nm plasmas, which continue to decay to 11 000 K by 2 μs. It is noted that the temperatures in the 355 nm plasmas are consistently higher than at other wavelengths. The reason for this difference is not known.

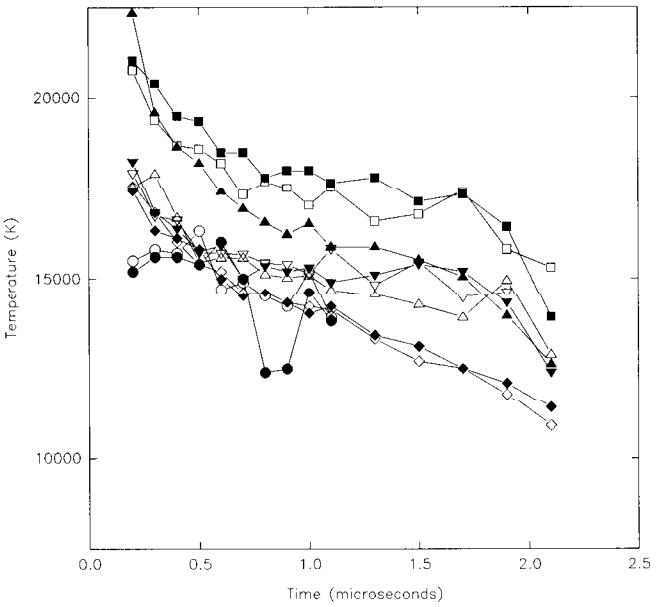

Fig. 4. Plot of the excitation temperature as a function of time in laser-produced plasmas formed in CO and CO_2 gases. *Open symbols:* CO; *filled symbols:* CO_2. *Circles:* 193 nm; *inverted triangles:* 266 nm; *squares:* 355 nm; *triangles:* 532 nm; *diamonds:* 1064 nm

In the case of the 1064 nm plasmas, the temperatures tend to be lower and to be decaying more rapidly than at other wavelengths, especially at later times in the plasma decay. It is believed that the lower temperatures observed are due to the use of a line-of-sight technique [4] which gives an average temperature over the viewed volume. The 1064 nm plasmas are larger, as evidenced visually and by the greater absorbed energies (6–7 mJ at 1064 nm), and the observed temperatures likely show some effects due to the outer portions of the plasma as it cools. However, due to the small dimension of the plasmas (< mm), spatial averaging is not likely to alter the determined values significantly, as observed by Radziemski et al. [4]. Otherwise, there are not significant differences in the temperatures of the plasma environments as a function of the laser wavelength.

Radziemski et al. have reported excitation temperatures for Nd:YAG and CO_2 laser-produced plasmas formed in air at 580 Torr [4, 25]. The temperatures range from 8 000 K to 16 000 K for Nd:YAG radiation (1064 nm) and 11 000 K to 19 000 K for CO_2 radiation with the highest temperatures recorded at the earliest

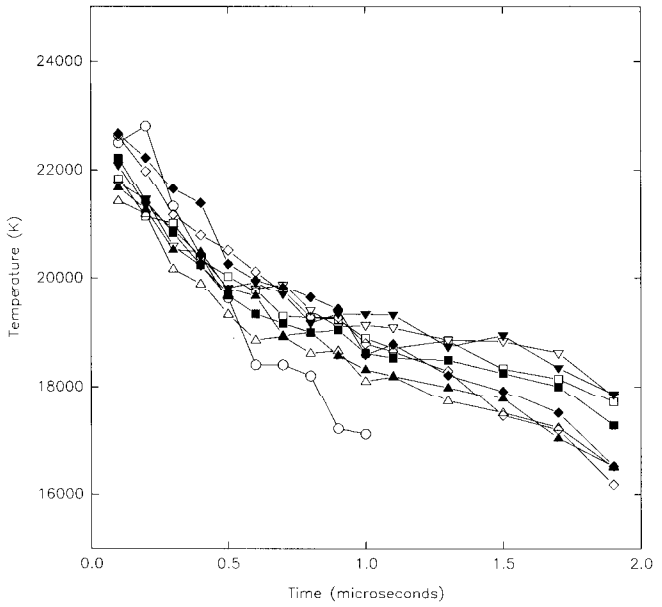

Fig. 5. Plot of the ionization temperature as a function of time in laser-produced plasmas formed in CO and CO_2 gases. *Open symbols:* CO; *filled symbols:* CO_2. *Circles:* 193 nm; *inverted triangles:* 266 nm; *squares:* 355 nm; *triangles:* 532 nm; *diamonds:* 1064 nm

decay times (approximately 1 μs in these cases). These values are very similar to the temperatures measured in the present study and are in excellent agreement with the temperatures measured at 1 μs, 14 000 K to 18 000 K.

2.4 *Ionization temperature*

Shown in Fig. 5 is a plot of the ionization temperatures as determined from the plasma emissions of carbon atoms (neutrals and ions) in Nd:YAG and ArF-laser plasmas formed in CO and CO_2 gases. Ionization temperatures shown at 193 nm using an ArF-excimer laser are taken from [13]. The observed carbon neutral emission line is at 247.856 nm corresponding to the $2p3s\ ^1P^0_1 \leftarrow 2p^2\ ^1S_0$ transition (61982–21648 cm^{-1}). The carbon ion lines observed are the multiplet at 251.1 nm corresponding to the $2p^3\ ^2D^0_{5/2} \leftarrow 2s2p^2\ ^2P_{3/2}$ transitions (150465–110652 cm^{-1}). Electron densities evaluated from the oxygen emissions at 844.65 nm (presented in Fig. 2) were used for the calculations of T_{ion}. Ionization temperatures were calculated using the Saha relationship as described previously [13]. Based on uncertainty in the oscillator strengths alone, uncertainty in the ionization temperatures is estimated to be 7% [13]. There is very close agreement of the various T_{ion} determinations at all wavelengths and in both CO and CO_2 gases at a common wavelength (no obvious chemical dependence). The T_{ion} values of CO reported previously for ArF laser plasmas are shown for comparison purposes. The trend is similar in all cases; a peak value for T_{ion} of approximately 22 000 K to 23 000 K is observed at 0.1 μs followed by a decrease to about 16 000 K to 17 000 K at 1–2 μs.

The good agreement of T_{ion} in the various plasmas is another demonstration of the similarity of these environments and does not indicate a spectral dependence of the plasma characteristics. It is possible, however, that with improved temporal resolution, spectral features in the plasma decay may show a dependence on the laser wavelength, especially in the initial stages of development (time < 100 ns).

The ionization temperatures observed in this study are consistent with those reported in other studies. Radziemski et al. reported ion temperatures in Nd:YAG laser-produced plasmas formed in air using carbon, nitrogen and beryllium as thermometric probe species [4]. In that study, T_{ion} ranged from 22 000 K to 16 000 K for nitrogen (0.5–2 μs), 20 000 K to 13 000 K for carbon (0.2–2 μs) and 13 000 K to 8 000 K for beryllium (1–30 μs). Stricker and Parker have reported peak ionization temperatures (observed in the first 15–20 ns) for Nd:YAG-laser-produced plasmas formed in 1.5 atm of oxygen of approximately 30 000 K [17]. The temperature of the plasma at later times was not reported.

2.5 *Equilibrium considerations*

In order to evaluate the temperature by the spectroscopic methods used in this study, it was necessary to assume the plasmas were in a state of LTE. There are several reasons to argue that this is a valid assumption. First, in determining whether a plasma is in a state of LTE, the velocity distribution of the free electrons should be Maxwellian. Griem [26] has stated that the velocity distribution of free electrons in dense plasmas (N_e more than 10^{16} cm^{-3}) of moderate temperature (kT less than 5 eV) is nearly always Maxwellian. A Maxwellian distribution is certainly expected for the CO and CO_2 laser-produced plasmas, since the plasma electron density ranges from nearly 10^{18} cm^{-3} at the earliest times to 10^{17} cm^{-3} at 2 μs with temperatures (T_{exc} and T_{ion}) of 2 eV or less.

In general terms, LTE is valid only if collision induced processes dominate over radiative decay and recombination processes. Since electronic collisions are by far the most frequent in a laser-produced plasma, the primary consideration is the magnitude of the electron density. For a given range of energy levels in a given species, LTE conditions are possible only if a minimum electron density is present. This minimum density can be estimated using the following expression [27, 28]:

$$N_e \gg 1.6 \times 10^{12} (T)^{1/2} (\Delta E)^3,$$

where N_e is in cm^{-3}, T is in K and E is in eV. For plasma temperatures of 2 eV (about 22 000 K) and N_e of 10^{18} cm^{-3}, LTE can be expected over a range of energies ΔE of 7–8 eV.

In the case of a transient plasma environment, such as a pulsed laser-produced plasma, the magnitude of the electron density indicates not only if LTE conditions are possible, but how quickly a plasma (once formed) will proceed towards LTE. The time needed to establish a kinetic equilibrium between electrons and heavier particles can be estimated using an expression from Lochte-Holtgreven [29].

$$t_{kin} = \left[7.5 \times 10^{-7} \left(\frac{X_H}{kT} \right)^{3/2} N_e \right]^{-1} \frac{nm}{n_+ m_e}$$

where k is Boltzmann's constant (in J/K), X_H is the ionization potential of hydrogen (in J), $n(n_+)$ is the number density of neutral (charged) species (in cm^{-3}), m is the atomic mass (in g) and m_e is the electron mass (in g). Using estimates of the initial plasma conditions (i.e., N_e of 10^{18} cm^{-3}, T_{exc} of 20 000 K, 99% ionized plasma), the time necessary to achieve a kinetic equilibrium between electrons and particles of up to mass 20 amu is on the order of nanoseconds.

Another consideration in a transient plasma environment is the time necessary for Boltzmann equilibration to take place once the plasma is formed. This can be estimated using another expression taken from Lochte-Holtgreven [29].

$$t_B = 1.1 \times 10^7 \frac{z^3}{f_{1,2} N_e} \frac{n_z}{n_z + n_{z-1}} \left(\frac{E_{z-1,2}}{z^2 X_H} \right) \times \left(\frac{kT}{z^2 X_H} \right)^{1/2} \exp \left(\frac{E_{z-1,2}}{kT} \right),$$

where z is the stage of ionization (1 = neutrals, 2 = singly charged, etc.), f is the oscillator strength, n_z is the density of the particles (in cm^{-3}), E_i is the energy of the state i (in J), and the rest are as previously. Under similar plasma conditions as described above (T_{exc} of 20 000 K and N_e of 10^{18} cm^{-3}), a Boltzmann equilibrium among the excited states of the different particles is expected within approximately 1 ns.

Although a LTE plasma should be characterized experimentally by a single temperature that simultaneously describes the Maxwell, Boltzmann and Saha distributions, such a single temperature was not observed in these studies. In fact, there appears to be a discrepancy between the excitation and ionization temperatures (T_{exc} and T_{ion}, respectively), which might suggest non-equilibrium conditions.

This apparent discrepancy is not believed to be significant, however, because of the relatively high degree of uncertainty associated with temperatures determined using the "two line" method, as was employed in these studies. The accuracy of this approach is usually limited by the uncertainty of the oscillator strengths of the observed transitions. The uncertainty of the temperature determined from the relative intensities of two emission wavelengths of the same species (of the same or adjacent ionization stages) can be estimated by the following expression [13, 29, 30]:

$$\frac{\Delta T}{T} = \frac{kT}{E_2 - E_1} \frac{\Delta R}{R},$$

where T is the temperature (in K), k is Boltzmann's constant (in J/K), E_i is the energy of the observed state (in J), and R is the ratio of measured emission intensities (I_2/I_1).

In the present studies, the uncertainty of the oscillator strengths of the O atom emissions at 777 nm and 795 nm are 10% and 25%, respectively [31], which limits the accuracy of the reported temperatures (for T approximately 20 000 K) to at best 15%, but possibly as high as 30%. Thus the observed T_{exc} and T_{ion}, which initially appear to disagree, are found to be in agreement within the estimated uncertainties at all but the earliest decay times. It follows that the discrepancies observed in the temperature plots are not in fact significant, nor are they an indication of non-LTE conditions.

Other studies of atmospheric pressure laser-produced plasmas reported in the literature have found experimental evidence of LTE. Radziemski et al. concluded that LTE was probable in Nd:YAG laser-produced plasmas formed in air by about 1 μs following the laser pulse [4]. They also found evidence of LTE conditions in CO_2-laser-produced plasmas formed in air at times greater than 10 μs [25]. Many of their arguments in support of LTE are also used here. Stricker and Parker inferred the existence of LTE from spectroscopic studies of optical breakdown in nitrogen and oxygen gases using a Nd:YAG laser at 1064 nm [17].

Further evidence for LTE can be found by comparing the results of this study with a model of an equilibrium CO_2 plasma reported by Dresvin [32]. Shown in Fig. 6 is a plot of plasma electron density versus plasma temperature which have been measured for Nd:YAG and ArF-laser-produced plasmas formed in CO_2 with those from Dresvin. The temperatures and corresponding densities were measured at 1.9 μs in the decay. The ionization temperature measurements are expected to be more accurate than the excitation temperatures [13, 29, 30], and are

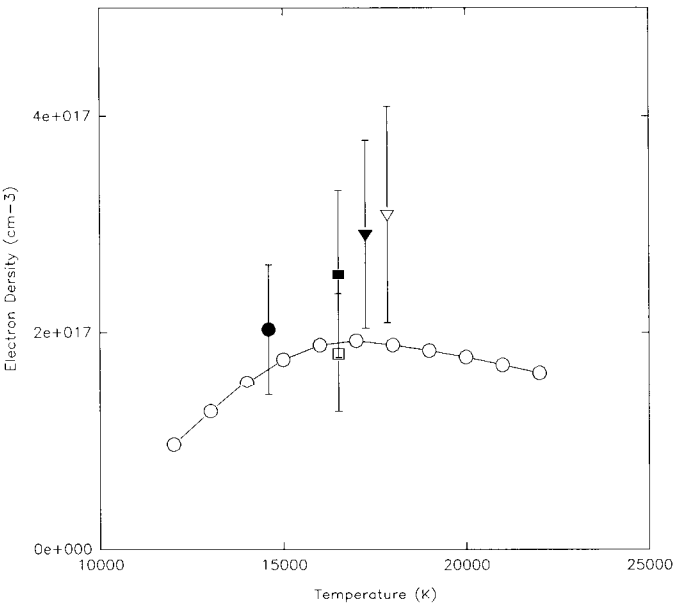

Fig. 6. Plot of the electron density as a function of temperature in laser-produced plasmas formed in CO_2. *Open circles:* model from Dresvin [30]; *filled circle:* 193 nm; *open inverted triangle:* 266 nm; *filled inverted triangle:* 355 nm; *open square:* 532 nm; *filled square:* 1064 nm

therefore shown in preference to excitation temperatures, except at 193 nm for which CO_2 ionization temperatures were not determined due to poor signal-to-noise. Error bars shown on the plot indicate the typical uncertainty (up to 30%) associated with the electron density when it is evaluated by the method used here [4, 24].

The plot shows good agreement between the model and experimentally determined values, although it does indicate that Nd:YAG- and ArF-laser-produced plasmas are characterized by an electron density slightly higher than is predicted by the model. Depending on the model's estimations of the physical properties of the plasma (e.g., partition function, ionization potential reduction, kinetic rates, etc.), it is possible the model underpredicts true equilibrium conditions of a CO_2 plasma at one atmosphere, as was suggested in [25], in which case the experimental results may be more correct. In either case, the agreement of the model and the experimental data indicates that the evaluated excitation and ionization temperatures are valid and are characteristic of the Boltzmann and Saha distributions in these laser-produced plasma environments.

It is interesting to speculate on the pressure characteristics of the laser-produced plasma environments. Although it is often possible to evaluate the pressure using the emission profiles, in the case of dense plasmas (such as laser-produced plasmas), the Stark broadening dominates the lineshapes preventing such determinations. It is possible, however, to estimate the pressure using the Saha, Dalton and charge equilibrium expressions together with knowledge of the plasma temperatures and electron density. By assuming complete atomization of the precursor species, and also assuming >99% ionization following breakdown, the equilibrium plasma pressure at 0.1 μs after the laser pulse is estimated to be 5.5 atm for an observed (ion) temperature of 22 000 K and density of 9×10^{17} cm^{-3}. At times later in the plasma decay, estimations of the total density become more speculative as the rates of recombination (ion-electron and molecular) are not well established, which limits the accuracy of estimating the ion/neutral and atom/molecule distributions. Indeed as Lochte-Holtgreven has discussed, in the case of a transient plasma it is best to measure the plasma pressure directly rather than inferring it using temperatures and equilibrium expressions [29].

However, if the plasma is assumed to be highly ionized at later times (e.g., 1 and 1.9 μs), the measured electron density and temperature at these times can continue to be used to estimate the plasma pressure. This assumption is not unjustified according to the model predictions of an equilibrium CO_2 plasma given by Dresvin [32]. At 1 μs, the ion temperature in the plasmas is approximately 19 000 K and the density is approximately 3×10^{17} cm^{-3}. At 1.9 μs in the plasma decay, the ion temperature is approximately 17 000 K and the electron density is approximately 2×10^{17} cm^{-3}. Again using the Dalton and charge equilibrium expressions, these conditions correspond to pressures of 1.5 atm at 1 μs and 0.93 atm at 1.9 μs, which is consistent with the ambient pressure in which the laser plasma is formed.

3 Conclusions

Intensity breakdown thresholds for air, CO and CO_2 at 1 atm have been measured at 193 nm, 266 nm, 355 nm, 532 nm and 1064 nm. A clear reduction of the breakdown threshold is observed for CO and CO_2 at 193 nm relative to thresholds at 266 nm, 355 nm, 532 nm and 1064 nm. This reduction is almost certainly due to resonance-enhanced two-photon ionization processes of metastable carbon atoms occurring at a wavelength of 193.093 nm, which is within the spectral bandpass of the ArF-laser output. Breakdown thresholds at 193 nm for these gases are approximately one order of magnitude less than at the other wavelengths and also less than in air at all wavelengths studied. A further reduction of the breakdown threshold is observed for CO at 193 nm (relative to CO_2) which has a favorable two-photon dissociation process resulting in rapid generation of carbon atoms in the laser focus.

Laser-produced plasmas produced in CO and CO_2 using the 266 nm, 355 nm, 532 nm and 1064 nm output of a Nd:YAG laser have also been studied using time-resolved emission spectroscopy to evaluate excitation temperatures, ionization temperatures and plasma electron densities, specifically for the purpose of determining differences in the plasmas due to changes in the laser wavelength. Current studies indicate that, aside from differences in the breakdown thresholds, there are no discernable differences in the resulting plasma environments as a function of the wavelengths used, nor are there differences due to the chemical structure of the plasma precursor gases. Dense, high temperature plasmas are formed which rapidly decay toward an equilibrium (or near-equilibrium) state. Maximum excitation temperatures are near 20 000 K, maximum ionization temperatures reach 23 000 K and maximum electron densities are near 10^{18} cm^{-3}. Kinetic and Boltzmann equilibration times are conservatively estimated to be on the order of 10 ns. For several reasons, the plasma environments are believed to reach LTE conditions. This is supported by agreement (within the uncertainty) of the excitation and ionization temperatures, comparisons with previous studies and comparisons with the predictions of an equilibrium model. The observed electron densities of the Nd:YAG laser plasmas are slightly higher than those predicted by the equilibrium model. Notwithstanding, Saha-Boltzmann equilibrium conditions are expected to exist allowing spectroscopic temperature determinations as have been performed.

Acknowledgements. The authors acknowledge partial support from US Air Force Office of Scientific Research Contract MIPR 91-0004 and support for equipment from the Productivity Investment Funding Program administered by Mr. David Ellis. J.B. Simeonsson gratefully acknowledges support from the US Army Research Laboratory through the National Research Council Postdoctoral Associateship Program.

References

1. G.M. Weyl: In *Laser-Induced Plasmas and Applications,* ed. by L.J. Radziemski, D.A. Cremers (Dekker, New York 1989) pp. 1–67
2. P. Shah, A. Biswas, R.L. Armstrong, L.J. Radziemski: J. Appl. Phys. **68,** 3809 (1990)
3. J.P. Davis, A.L. Smith, C. Giranda, M. Squicciarini: Appl. Opt. **30,** 4358 (1991)
4. L.J. Radziemski, T.R. Loree, D.A. Cremers, N.M. Hoffman: Anal. Chem. **55,** 1246 (1983)
5. M. Casini, M.A. Harith, V. Palleschi, A. Salvetti, D.P. Singh, M. Vaselli: Laser Part. Beams **9,** 633 (1991)
6. L.J. Radziemski, D.A. Cremers: In *Laser-Induced Plasmas and Applications,* ed. by L.J. Radziemski, D.A. Cremers (Dekker, New York 1989) pp. 295–325
7. V. Majidi, M.R. Joseph: CRC Crit. Rev. Anal. Chem. **23,** 143 (1992)
8. K. Niemax, W. Sdorra: Appl. Opt. **29,** 5000 (1990)
   X.Z. Zhao, L.J. Shen, T.X. Lu, K. Niemax: Appl. Phys. B **55,** 327 (1992)
9. D.A. Cremers, L.J. Radziemski, T.R. Loree: Appl. Spectrosc. **38,** 721 (1984)
   J.R. Wachter, D.A. Cremers: Appl. Spectrosc. **41,** 1042 (1987)
10. D.C. Smith, R.G. Meyerand: In *Principles of Laser Plasmas,* ed. by G. Bekefi, (Wiley, New York 1976) pp. 458–478, 464, and references therein
11. Yu. P. Raizer: *Laser-Induced Discharge Phenomena* (Plenum, New York 1977)
12. C. Grey-Morgan: Rep. Prog. Phys. **38,** 621 (1975)
13. J.B. Simeonsson, A.W. Miziolek: Appl. Opt. **32,** 939 (1993)
14. R. Tambay, R.K. Thareja: J. Appl. Phys. **70,** 2890 (1991)
15. R.J. Locke, J.B. Morris, B.E. Forch, A.W. Miziolek: Appl. Opt. **29,** 4987 (1990)
16. J.B. Morris, B.E. Forch, A.W. Miziolek: Appl. Spectrosc. **44,** 1040 (1990)
17. J. Stricker, J.G. Parker: J. Appl. Phys. **53,** 851 (1982)
18. R.A. Armstrong, R.A. Lucht, W.T. Rawlins: Appl. Opt. **22,** 1573 (1983)
19. R.C. Sausa, A.J. Alfano, A.W. Miziolek: Appl. Opt. **26,** 3588 (1987)
20. H.F. Döbele, B. Rückle: J. Nucl. Mater. **111/112,** 102 (1982)
21. H.F. Döbele, B. Rückle: Plasma Phys. **24,** 1419 (1982)
22. B.E. Forch, C.N. Merrow: J. Chem. Phys. **95,** 3252 (1991)
23. H.R. Griem: *Spectral Line Broadening by Plasmas* (Academic, New York 1974) pp. 170–211, 226–231, 320–337
24. W.L. Wiese: In *Plasma Diagnostic Techniques,* ed. by R.H. Huddlestone, S.L. Leonard (Academic, New York 1965) pp. 265–317
25. L.J. Radziemski, D.A. Cremers, T.M. Niemczyk: Spectrochim. Acta **40B,** 517 (1985)
26. H.R. Griem: Phys. Rev. **131,** 1170 (1963)
27. A.P. Thorne: *Spectrophysics,* 2nd edn. (Chapman and Hall, London 1988) pp. 355–358
28. P.K. Carroll, E.T. Kennedy: Contemp. Phys. **22,** 61 (1981)
29. W. Lochte-Holtgreven: In *Plasma Diagnostics,* ed. by W. Lochte-Holtgreven (North-Holland, Amsterdam 1968) pp. 146–156, 180–184
30. G. Bekefi, C. Deutsch, B. Yaakobi: In *Principles of Laser Plasmas,* ed. by G. Bekefi (Wiley, New York 1976) pp. 592–594
31. W.L. Wiese, M.W. Smith, B.M. Glennon: *Atomic Transition Probabilities,* Vol. 1 NSRDS-NBS-4 (NBS, Washington, DC 1966)
32. S.V. Dresvin: *Physics and Technology of Low-Temperature Plasmas,* ed. by H.U. Eckert (Iowa-State Univ. Press, Ames, IA 1977) pp. 18–24